Rank-One Matrix Approximation With ℓ_p-Norm for Image Inpainting

Xiao Peng Li, Qi Liu, and Hing Cheung So, *Fellow, IEEE*

***Abstract*—In the problem of image inpainting, one popular approach is based on low-rank matrix completion. Compared with other methods which need to convert the image into vectors or dividing the image into patches, matrix completion operates on the whole image directly. Therefore, it can preserve latent information of the two-dimensional image. An efficient method for low-rank matrix completion is to employ the matrix factorization technique. However, conventional low-rank matrix factorization-based methods often require a prespecified rank, which is challenging to determine in practice. The proposed method factorizes an image matrix as a sum of rank-one matrices so that it does not require rank information in advance as it can be automatically estimated by the algorithm itself when the algorithm has satisfactorily converged. In our study, matching pursuit is applied to search for the best rank-one matrix at each iteration. To be robust against impulsive noise, the residual error between the observed and estimated matrices is minimized by ℓ_p-norm with $0 < p < 2$. Then the resultant ℓ_p-norm minimization is solved by the iteratively reweighted least squares method. The proposed model is beneficial for the robustness against outliers, and does not require rank information. Experimental results verify the effectiveness and higher accuracy of the proposed method with comparison to several state-of-the-art matrix completion-based image inpainting approaches.**

***Index Terms*—Image inpainting, low-rank matrix completion, outlier-robustness, ℓ_p-minimization, matching pursuit.**

I. Introduction

IMAGE inpainting is a fundamental task in image processing, which is a restoration procedure where damaged, deteriorating, or missing parts of a digital image are reconstructed. With the recent development in image processing techniques, it has been gained even more popularity. One class of image inpainting approaches is based on patch processing, including [1]-[4], where the impaired image is divided into a number of patches which are small areas of the whole image. Ultimately the restored image is constructed by combining all these individual results. The above operation has one major defect that the processing is imposed on intermediate (patch) results, rather than on the whole image, which may miss latent information. In addition, these methods are at the cost of high computational cost and memory usage.

Another type of image inpainting methods operates on the whole image directly, which restores pixels via the low-rank matrix completion technique. The matrix completion method can retain the potentially two-dimensional information of the target image. A variety of matrix completion techniques for image inpainting have been proposed, such as singular value thresholding (SVT) [10], fixed point continuation (FPC) [11], accelerated proximal gradient descent (APG) [12] and truncated nuclear norm regularization (TNNR) [8]. Since these methods require computing full (or truncated) singular value decomposition (SVD) at each iteration, they are computationally demanding, especially for processing large-size images. To decrease computational complexity, approaches based on low-rank matrix factorization are proposed, such as low-rank matrix fitting (LMaFit) [13], alternating minimization for matrix completion (AltMinComplete) [14] and subspace evolution and transfer (SET) [15]. They convert the estimated matrix as a product of two matrices which have much smaller dimensions. However, they require a prior rank information of the observed matrix, and determining the rank of a real-world image matrix is difficult in practice. To address this issue, rank-one matrix completion with ε (R1MC-ε) [16] and rank-one matrix completion (R1MC) [30] have been proposed to factorize the estimated matrix into a sum of rank-one matrices and employ ℓ_1-norm to automatically estimate the matrix rank. It is worth noting that the above methods rely on the assumption of noise-free or Gaussian noise since their algorithm development is based on the ℓ_2-space optimization. The presence of outliers may lead to serious degradation of inpainting performance. Accordingly, algorithms based on ℓ_p-norm with $0 < p < 2$ are proposed, such as alternating projection (AP) [17], ℓ_p-regression (ℓ_p-reg) [23] and variational Bayesian matrix factorization based on L1-norm (VBMFL1) [19]. Nevertheless, AP requires predicting a prior noise factor on ℓ_p-norm in advance, which is difficult to achieve in practice. Regarding ℓ_p-reg, it needs the matrix rank information. Another robust matrix completion approach is proximal alternating robust subspace minimization (PARSuMi) [18]. It also requires a prior parameter, that is, the upper bound of the number of outliers.

In this work, motivated by rank-one matrix approximation, we devise a simple and efficient matrix completion algorithm for image inpainting. Different from conventional methods, it is not only robust to outliers, but also does not require rank or noise information. Primarily, the estimated matrix is approximated

Manuscript received February 9, 2020; revised April 11, 2020; accepted April 11, 2020. Date of publication April 20, 2020; date of current version May 19, 2020. The associate editor coordinating the review of this manuscript and approving it for publication was Prof. Mylene Q Farias. *(Corresponding author: Qi Liu.)*

Xiao Peng Li and Hing Cheung So are with the Department of Electrical Engineering, City University of Hong Kong, Kowloon Tong, Hong Kong (e-mail: x.p.li@my.cityu.edu.hk; hcso@ee.cityu.edu.hk).

Qi Liu is with the Department of Electrical and Computer Engineering, National University of Singapore, Singapore 119260, Singapore (e-mail: elelqi@nus.edu.sg).

Digital Object Identifier 10.1109/LSP.2020.2988596

as a sum of rank-one matrices in the proposed model. Then, we employ ℓ_p-norm with $0 < p < 2$ to minimize the residual between the given matrix and estimated matrix, which enables robustness. In each iteration, we use greedy pursuit to search for the optimal rank-one matrix, where the rank-one matrix is represented by a product of two vectors. Last but not the least, our model can be implemented in a distributed or parallel manner, which can greatly reduce computing time with multiple terminals or threads.

II. Problem Formulation

For a gray-scale image, it can be mathematically represented as a matrix, defined as $\boldsymbol{X} \in \mathbb{R}^{m\times n}$. Assume there are some missing pixels (holes) in the incomplete matrix $\boldsymbol{X}_\Omega$, it is modeled as:

$$\boldsymbol{X}_\Omega = \boldsymbol{X} \odot \Omega \tag{1}$$

Herein, $\odot$ is the element-wise multiplication operator. $\Omega \in \mathbb{R}^{m\times n}$ is a binary matrix comprised of 0 and 1, where 0 and 1 mean those entries in $\boldsymbol{X}_\Omega$ are missing and known, respectively. It has been studied that the image matrix has an approximately low-rank structure [8]. Therefore, given an incomplete image matrix $\boldsymbol{X}_\Omega$ containing noise, the image inpainting problem can be formulated as:

$$\min_{\boldsymbol{M}} \text{rank}(\boldsymbol{M}), \text{ s.t. } ||\boldsymbol{X}_\Omega - \boldsymbol{M}_\Omega||_F \le \delta \tag{2}$$

where $||\cdot||_F$ denotes the Frobenius norm of a matrix, and $\delta > 0$ is a tolerance parameter to balance the fitting error. Unfortunately, the rank minimization problem is NP-hard in general since the rank is discrete and nonconvex. To handle this issue, nuclear norm minimization is proposed to relax rank minimization [9], which is analogous to the strategy of approximating the ℓ_0-norm by ℓ_1-norm in compressed sensing [5]. In [6], it is verified that the nuclear norm is the convex envelope of rank. Whereafter, Candès and Tao have proved that one can solve the matrix completion problem via minimizing nuclear norm with a high probability [7]. Hence, (2) is approximately transformed to:

$$\min_{\boldsymbol{M}} ||\boldsymbol{M}||_*, \text{ s.t. } ||\boldsymbol{X}_\Omega - \boldsymbol{M}_\Omega||_F \le \delta \tag{3}$$

where $||\cdot||_*$ represents the nuclear norm of a matrix, that is, the sum of all singular values of the matrix. There are many state-of-the-art approaches proposed to deal with (3). The first class is to solve (3) directly via computing SVD, including SVT, FPC, APG, to name just a few which do not require rank information. However, it is well known that computing SVD will pay an expensive computational cost. Another popular category is based on the matrix factorization technique, which can avoid SVD computation but they require rank information, corresponding to the following optimization:

$$\min_{\boldsymbol{U},\boldsymbol{V}} ||\boldsymbol{X}_\Omega - (\boldsymbol{UV})_\Omega||_F^2 \tag{4}$$

where $\boldsymbol{U} \in \mathbb{R}^{m\times r}$ and $\boldsymbol{V} \in \mathbb{R}^{r\times n}$ with r being the rank of the target matrix. Then, the target matrix can be calculated by $\boldsymbol{M} = \boldsymbol{UV}$ after determining $\boldsymbol{U}$ and $\boldsymbol{V}$. However, impulsive noise appears in many practical scenarios, such as salt-and-pepper noise in an image. It is well known that ℓ_2-space optimization cannot resist impulsive noise effectively. In contrast, ℓ_p-norm is able to resist impulsive noise since it reduces the effect of outliers via calculating the residual to power of p with $0 < p < 2$. To be robust against impulsive noise, Zeng and So [23] replace Frobenius norm by ℓ_p-norm, leading to:

$$\min_{\boldsymbol{U},\boldsymbol{V}} ||\boldsymbol{X}_\Omega - (\boldsymbol{UV})_\Omega||_p^p \tag{5}$$

where $||\cdot||_p^p$ of a matrix $\boldsymbol{E}$ is defined as $||\boldsymbol{E}||_p^p = \sum_{i,j} |[\boldsymbol{E}]_{ij}|^p$. However, (4) and (5) are based on an ideal assumption that we have known the rank of the observed matrix.

III. ℓ_p-Norm Matching Pursuit

Given $\boldsymbol{M} \in \mathbb{R}^{m\times n}$, it can be decomposed into a linear combination of rank-one matrices, that is:

$$\boldsymbol{M} \approx \sum_{k=1}^{K} \boldsymbol{M}_k \tag{6}$$

where $\boldsymbol{M}_k = \boldsymbol{u}_k\boldsymbol{v}_k^T$ [22] with $\boldsymbol{u}_k \in \mathbb{R}^m$ and $\boldsymbol{v}_k \in \mathbb{R}^n$, and the target rank K is equal to the number of iterations when the proposed method converges, where convergence means that residual $\boldsymbol{R}_k$ (defined below) decreases very slowly. Then, to achieve robustness to impulsive noise, (4) combined with ℓ_p-norm is rewritten as:

$$\min_{\boldsymbol{M}} ||\boldsymbol{X}_\Omega - \boldsymbol{M}_\Omega||_p^p \tag{7}$$

Wang *et al.* have proposed to utilize the greedy pursuit method to solve (7) with $p = 2$ [27]. In our work, we employ greedy pursuit to tackle (7) with $0 < p < 2$ which can search for the best rank-one basis matrix of the current residual $\boldsymbol{R}_k$ at the kth iteration, which is formulated as:

$$\min_{\boldsymbol{u}_k,\boldsymbol{v}_k} ||\boldsymbol{R}_k - (\boldsymbol{u}_k\boldsymbol{v}_k^T)_\Omega||_p^p \tag{8}$$

where $\boldsymbol{R}_k = \boldsymbol{X}_\Omega - (\sum_{i=1}^{k-1} \boldsymbol{u}_i\boldsymbol{v}_i^T)_\Omega$ with $k \ge 2$ and $\boldsymbol{R}_1 = \boldsymbol{X}_\Omega$. In the following, we adopt the alternating minimization method [23] to solve $\boldsymbol{u}_k$ and $\boldsymbol{v}_k$ and omit k for the sake of presentation simplicity. Firstly, we fix variable $\boldsymbol{v}$ and then optimize $\boldsymbol{u}$, resulting in:

$$\boldsymbol{u}^q = \arg\min_{\boldsymbol{u}} ||\boldsymbol{R} - (\boldsymbol{u}(\boldsymbol{v}^{q-1})^T)_\Omega||_p^p \tag{9}$$

where q means the qth iteration in the alternating minimization process. Define $(\boldsymbol{r}_i)^T \in \mathbb{R}^n$ and $(u_i)^q$ as the ith row of $\boldsymbol{R}$ and the ith entry of $\boldsymbol{u}^q$, respectively. Since each $(u_i)^q$ is determined by $(\boldsymbol{r}_i)^T$ and $(\boldsymbol{v}^{q-1})^T$, (9) is equivalent to solving the following m independent sub-problems:

$$(u_i)^q = \arg\min_{u_i} ||(\boldsymbol{r}_i)^T - (u_i(\boldsymbol{v}^{q-1})^T)_{\mathcal{I}_i}||_p^p \tag{10}$$

where $\mathcal{I}_i \in \mathbb{R}^n$ denotes the ith row of Ω. Because $\boldsymbol{R}_k = \boldsymbol{X}_\Omega - (\sum_{i=1}^{k-1} \boldsymbol{u}_i\boldsymbol{v}_i^T)_\Omega$, $(\boldsymbol{r}_i)^T = ((\boldsymbol{r}_i)^T)_{\mathcal{I}_i}$. It is easy to find that the residual between $((\boldsymbol{r}_i)^T)_{\mathcal{I}_i}$ and $((u_i(\boldsymbol{v}^{q-1})^T)_{\mathcal{I}_i}$ is only affected by all known elements in $((\boldsymbol{r}_i)^T)_{\mathcal{I}_i}$ and $(\boldsymbol{v}^{q-1})^T)_{\mathcal{I}_i}$. Therefore, (10) can be simplified as:

$$(u_i)^q = \arg\min_{u_i} ||(\boldsymbol{a}_i)^T - u_i\boldsymbol{b}^T||_p^p \tag{11}$$

where $(\boldsymbol{a}_i)^T \in \mathbb{R}^{||\mathcal{I}_i||_1}$ and $\boldsymbol{b}^T \in \mathbb{R}^{||\mathcal{I}_i||_1}$ only contain known entries in $(\boldsymbol{r}_i)^T$ and $(\boldsymbol{v}^{q-1})^T$, respectively, without changing

Algorithm 1: ℓ_p-MP for Matrix Completion.

Input: $\boldsymbol{X}_\Omega$
  Initialize: $\boldsymbol{R}_1 = \boldsymbol{X}_\Omega$, and randomize $\boldsymbol{v}_0$
  for $k = 1, 2, \cdots$ **do**
    1) $\boldsymbol{v}_k^0 = \boldsymbol{v}_{k-1}$
    for $q = 1, 2, \cdots$ **do**
      2) Calculate $\boldsymbol{u}_k^q = \arg\min_{\boldsymbol{u}_k} ||\boldsymbol{R}_k - (\boldsymbol{u}_k(\boldsymbol{v}_k^{q-1})^T)_\Omega||_p^p$
      3) Calculate $\boldsymbol{v}_k^q = \arg\min_{\boldsymbol{v}_k} ||\boldsymbol{R}_k - (\boldsymbol{u}_k^q \boldsymbol{v}_k^T)_\Omega||_p^p$
    end for
    4) $\boldsymbol{R}_{k+1} = \boldsymbol{R}_k - (\boldsymbol{u}_k(\boldsymbol{v}_k)^T)_\Omega$
    Stop if stopping criterion is met.
  end for
Output: $\boldsymbol{M} = \sum_{i=1}^k \boldsymbol{u}_i \boldsymbol{v}_i^T$

the order of entries where $||\cdot||_1$ is the ℓ_1-norm of a vector. Keeping the order of elements means from $(\boldsymbol{r}_i)^T = [1, 0, 3, 0, 2]$ to $(\boldsymbol{a}_i)^T = [1, 3, 2]$ with $\mathcal{I}_i = [1, 0, 1, 0, 1]$.

For $1 \leq p < 2$, (11) can be efficiently solved by the iteratively reweighted least squares (IRLS) method [25], [26] which provides global convergence. While for $0 < p < 1$, it only searches for a stationary point. At the tth inner iteration of IRLS, it solves a weighted LS problem as follows:

$$((u_i)^q)^{t+1} = \arg\min_{(u_i)^q} ||((\boldsymbol{a}_i)^T - (u_i)^q \boldsymbol{b}^T)\boldsymbol{w}^t||_2^2 \tag{12}$$

where $\boldsymbol{w}^t \in \mathbb{R}^{||\mathcal{I}_i||_1}$, and the nth element of $\boldsymbol{w}^t$ is calculated as $w_n^t = 1/(|\tau_n^t|^{\frac{2-p}{2}})$ with τ_n^t being the nth element of the residual vector $\boldsymbol{\tau}^t = (\boldsymbol{a}_i)^T - ((u_i)^q)^t \boldsymbol{b}^T$ with $((u_i)^q)^0 = \boldsymbol{b}^T\boldsymbol{a}_i/\boldsymbol{b}^T\boldsymbol{b}$. In the IRLS, the computational complexity is $\mathcal{O}(||\mathcal{I}_i||_1 T)$ for each $(u_i)^q$ where T is the iteration number to converge. Note that T is independent from the dimension of $\boldsymbol{X}_\Omega$ and with a value of several tens [25]. Therefore, the complexity for solving (9) is $\mathcal{O}(||\Omega||_1 T)$ with $||\Omega||_1 \ll mn$ because $\sum_{i=1}^m ||\mathcal{I}_i||_1 = ||\Omega||_1$.

Next, we optimize $\boldsymbol{v}$ via fixing $\boldsymbol{u}$. Specifically, we have:

$$\boldsymbol{v}^q = \arg\min_{\boldsymbol{v}} ||\boldsymbol{R} - (\boldsymbol{u}^q \boldsymbol{v}^T)_\Omega||_p^p \tag{13}$$

Because of the same structure of (9) and (13), $\boldsymbol{v}$ can be updated by a similar manner, with the following n independent subproblems:

$$(v_j)^q = \arg\min_{v_j} ||(\boldsymbol{r}_j)_{\mathcal{J}_j} - (v_j \boldsymbol{u}^q)_{\mathcal{J}_j}||_p^p \tag{14}$$

where $v_j, \boldsymbol{r}_j \in \mathbb{R}^m$ and $\mathcal{J}_j \in \mathbb{R}^m$ are the jth element of $\boldsymbol{v}$, the jth column of $\boldsymbol{R}$ and the jth column of Ω, respectively. After removing missing elements in $\boldsymbol{r}_j$ and $\boldsymbol{u}$, (14) is rewritten as:

$$(v_j)^q = \arg\min_{v_j} ||\boldsymbol{c}_j - v_j \boldsymbol{d}||_p^p \tag{15}$$

where both $\boldsymbol{c}_j$ and $\boldsymbol{d} \in \mathbb{R}^{||\mathcal{J}_j||_1}$. (15) can be solved by IRLS as well. The complexity for solving (13) is also $\mathcal{O}(||\Omega||_1 T)$. Hence, the total complexity is $\mathcal{O}(K||\Omega||_1 TQ)$ with $K \ll \min(m, n)$ where Q is the number of iterations for alternating minimization. Empirically, Q with the value of several tens satisfies convergence. Moreover, a distributed or parallel realization can be applied to solving $\boldsymbol{u}$ and $\boldsymbol{v}$. The processing time will sharply decrease via multiple terminals or threads.

All steps of the proposed method are summarized in Algorithm 1, which is referred to ℓ_p-matching pursuit (ℓ_p-MP). In this work, we define $\mathrm{E}(\boldsymbol{u}_k^q, \boldsymbol{v}_k^q) = \|\boldsymbol{R}_k - \boldsymbol{u}_k^q(\boldsymbol{v}_k^q)^T\|_p^p / \|\boldsymbol{R}_k\|_p^p$ and $\sigma = \mathrm{E}(\boldsymbol{u}_k^q, \boldsymbol{v}_k^q) - \mathrm{E}(\boldsymbol{u}_k^{q+1}, \boldsymbol{v}_k^{q+1})$. The smaller value of $\mathrm{E}(\boldsymbol{u}_k^q, \boldsymbol{v}_k^q)$ is, the closer $\boldsymbol{u}_k^q(\boldsymbol{v}_k^q)^T$ is to $\boldsymbol{R}_k$. If σ is less than 10^{-5}, we say that $\boldsymbol{u}_k$ and $\boldsymbol{v}_k$ have satisfactorily converged at the qth iteration. For the outer iteration, the convergence condition is $\eta = ||\boldsymbol{R}_k||_p^p / ||\boldsymbol{X}_\Omega||_p^p - ||\boldsymbol{R}_{k+1}||_p^p / ||\boldsymbol{X}_\Omega||_p^p \leq 5 \times 10^{-4}$.

The convergence of ℓ_p-MP is studied in the following proposition. Beforehand, we introduce the concept of ℓ_p-correlation [29], defined as $\theta_p(\boldsymbol{a}, \boldsymbol{b}) = 1 - \frac{\min_{\alpha\in\mathbb{R}} \|\boldsymbol{b} - \alpha\boldsymbol{a}\|_p^p}{\|\boldsymbol{b}\|_p^p}$. It is easy to know that $0 \leq \theta_p(\boldsymbol{a}, \boldsymbol{b}) \leq 1$ and $\min_{\alpha\in\mathbb{R}} \|\boldsymbol{b} - \alpha\boldsymbol{a}\|_p^p = (1 - \theta_p(\boldsymbol{a}, \boldsymbol{b}))\|\boldsymbol{b}\|_p^p$.

Proposition 1: The residual error of matching pursuit, defined as $\boldsymbol{R}_k$, is monotonically non-increasing with a lower bound, therefore it is convergent to a limit point.

Proof: Minimizing $\|\boldsymbol{R}_k - \boldsymbol{u}_k \boldsymbol{v}_k^T\|_p^p$ with respect to $\boldsymbol{u}_k$ at the kth iteration, we have:

$$\begin{aligned}\min_{\boldsymbol{u}} \|\boldsymbol{R}_k - \boldsymbol{u}\boldsymbol{v}_{k-1}^T\|_p^p &= \sum_{i=1}^m \min_{u_i} ||\boldsymbol{r}_i - (u_i(\boldsymbol{v}_{k-1})^T)||_p^p \\ &= \sum_{i=1}^m (1 - \theta_p(\boldsymbol{v}_{k-1}, \boldsymbol{r}_i))\|\boldsymbol{r}_i\|_p^p \\ &\leq \sum_{i=1}^m \|\boldsymbol{r}_i\|_p^p = \|\boldsymbol{R}_k\|_p^p\end{aligned}$$

Note that $\boldsymbol{v}_{k-1}$ is random due to random initialization. We obtain $\min_{\boldsymbol{v}} \|\boldsymbol{R}_k - \boldsymbol{u}_k \boldsymbol{v}^T\|_p^p \leq \|\boldsymbol{R}_k\|_p^p$ via minimizing $\|\boldsymbol{R}_k - \boldsymbol{u}_k \boldsymbol{v}_k^T\|_p^p$ with respect to $\boldsymbol{v}_k$ at the kth iteration in the same way. Hence, $\|\boldsymbol{R}_{k+1}\|_p^p = \min_{\boldsymbol{u}_k, \boldsymbol{v}_k} \|\boldsymbol{R}_k - \boldsymbol{u}_k \boldsymbol{v}_k^T\|_p^p \leq \|\boldsymbol{R}_k\|_p^p$. ∎

This means the residual error $\boldsymbol{R}_k$ does not increase at each iteration. Moreover, its lower bound is 0. Therefore, MP based on ℓ_p-norm is convergent. Moreover, the convergence of ℓ_p-norm minimization has been proved by the *Proposition 1* in [28]. Combining the results from the convergence analysis of MP and ℓ_p-norm minimization, it is verified that ℓ_p-MP is convergent.

Compared with ℓ_p-reg, their operations are different although ℓ_p-MP and ℓ_p-reg employ the IRLS method to optimize the ℓ_p-norm of residual. Herein, ℓ_p-MP utilizes IRLS to search for a scalar, while, IRLS is used to calculate a vector in ℓ_p-reg. Moreover, ℓ_p-MP does not require rank information, however calculating a rank is a prerequisite for ℓ_p-reg.

IV. Experimental Results

We adopt three images from [20], [21]. The salt-and-pepper noise is generated by the function “imnoise($\tilde{\boldsymbol{X}}$, ‘salt & pepper’, ρ)” in MATLAB, where $\tilde{\boldsymbol{X}}$ is the image matrix, ρ is the normalized noise intensity which is related to signal-to-noise (SNR) as $\rho = 1/\mathrm{SNR}$. Peak signal-to-noise ratio (PSNR) is widely used to evaluate the quality of a restored image, which is defined as:

$$\mathrm{PSNR} = 10 \times \log_{10}\left(\frac{(2^b - 1)^2}{\mathrm{MSE}}\right) \tag{16}$$

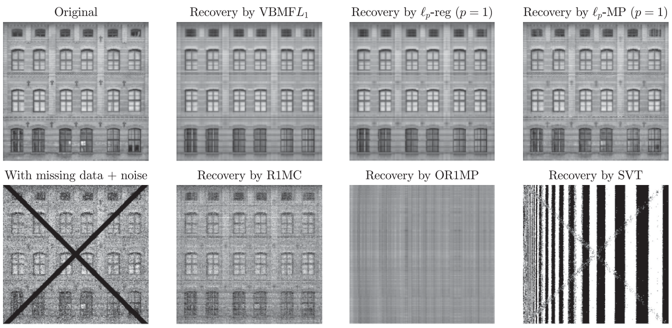

Fig. 1. Noisy image with missing data and recovered images.

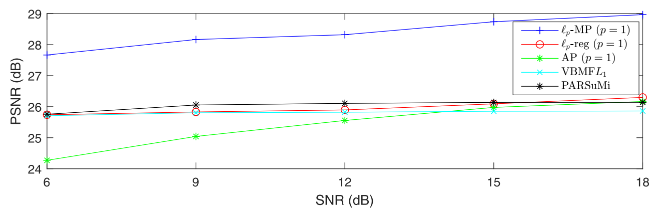

Fig. 2. PSNR versus SNR in salt-and-pepper noise.

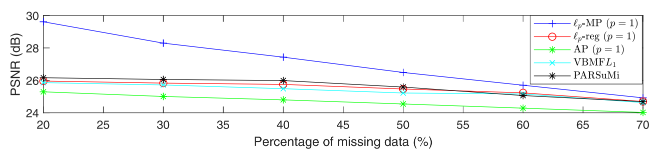

Fig. 3. PSNR versus percentage of missing data in salt-and-pepper noise at SNR $= 9$ dB.

where $b = 8$ is the number of bits per sample value, and MSE $= \frac{1}{mn}||\hat{\boldsymbol{X}} - \boldsymbol{X}||_F^2$ is the mean square error.

We compare the performance of ℓ_p-MP with ℓ_p-reg, AP, VBMFL_1, PARSuMi, SVT, R1MC and OR1MP [27]. Simulation results on the first image are shown in Fig. 1, where SNR = 5dB. The best rank used in ℓ_p-reg and VBMFL_1 is 6 [23]. SVT, R1MC and OR1MP are not robust to salt-and-pepper noise and they fail in restoring the image. Obviously, ℓ_p-MP, ℓ_p-reg, and VBMFL_1 can obtain a satisfactory result. However, the VBMFL_1 is still inferior to ℓ_p-reg with $p = 1$ since VBMFL_1 does not restore lamps on the wall. The proposed method is better than ℓ_p-reg with $p = 1$ from observing the bottom row of windows. For the recovered image from ℓ_p-MP, lamps on the wall are still a little fuzzy. The PSNRs of ℓ_p-MP, ℓ_p-reg and VBMFL_1 are 27.21dB, 25.84dB, and 25.71dB, respectively.

The performance of the proposed method versus SNR is plotted in Fig. 2, where 30% elements are missing. Since R1MC, OR1MP and SVT are not robust to impulsive noise, the corresponding results are not included. 6 is also the best rank of the first image for AP and PARSuMi [23]. We see that the proposed method performs best in the case of impulsive noise with higher PSNR compared with others.

The impact of the percentage of missing data is also investigated. Fig. 3 shows the PSNR versus the percentage of missing data. We see that the PSNR of ℓ_p-MP is higher than the others from 20% to 70%. In particular, ℓ_p-MP is prominent at a low percentage of missing data.

The impact of p is studied in Fig. 4. It is seen that the proposed method with $p = 1.2$ has the highest PSNR for different levels

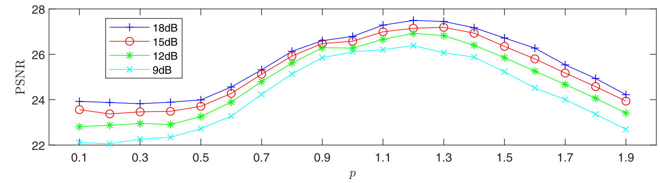

Fig. 4. PNSR versus p in different levels of salt-and-pepper noise with 50% missing data.

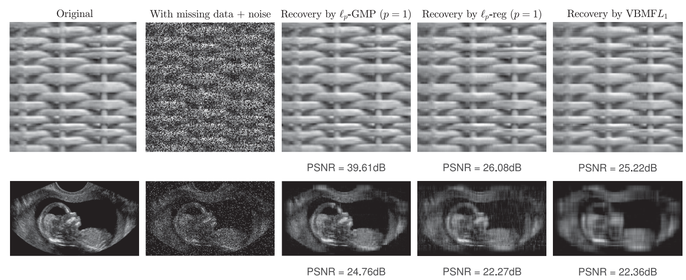

Fig. 5. Different noisy images with missing values and recovered results with different methods.

of salt-and-pepper noise. Note that this consequence is expected to be universal for image data which is normalized to the range from 0 to 1 since the impact of p is affected by the amplitude of impulsive noise which is a fixed value (0 or 1) for salt-and-pepper noise. The reason why we adopt $p = 1$ in ℓ_p-MP is to keep consistent with the value of p in AP and ℓ_p-reg. We also see the performance that of $0 < p < 1$ is worse than that of $p = 1$. A possible explanation regarding the inferiority of using a smaller value of p is that the corresponding ℓ_p-norm is non-convex and non-smooth, leading to poorer local solutions.

We then test other images. The best rank of the first image for ℓ_p-reg and VBMFL_1 is set to 6 [23]. After extensive trials, the best ranks of the second image are determined as 15 and 10 for ℓ_p-reg and VBMFL_1, respectively. Fig. 5 shows the original images, images with 40% missing information and salt-and-pepper noise at SNR $=$ 9dB, and recovered images from various methods. Note that the results of SVT, R1MC and OR1MP are not included since they are robust to impulsive noise. The PSNRs of the recovered image are shown at the bottom of each recovered image. It is observed that the proposed algorithm is the most robust to impulsive noise and yields the best recovery performance in terms of PSNR.

V. Conclusion

Many conventional matrix completion-based methods for image inpainting require the SVD computation, and/or user-defined parameters (e.g. rank and bound of outliers). To overcome these issues, we have combined greedy pursuit, low-rank matrix factorization and ℓ_p-norm minimization with $0 < p < 2$ to devise a computationally efficient algorithm for image inpainting. We model the estimated matrix as a sum of rank-one matrices, and then minimize ℓ_p-norm of residual error between the observed and estimated matrices. Simulation results demonstrate that the ℓ_p-MP algorithm is superior to the AP, ℓ_p-reg, VBMFL_1 and PARSuMi in terms of recovery performance and outlier-robustness.

REFERENCES

[1] K. Dabov, A. Foi, V. Katkovnik, and K. Egiazarian, "Image denoising by sparse 3-D transform-domain collaborative filtering," *IEEE Trans. Image Process.*, vol. 16, no. 8, pp. 2080–2095, Aug. 2007.

[2] W. Dong, L. Zhang, G. Shi, and X. Li, "Nonlocally centralized sparse representation for image restoration," *IEEE Trans. Image Process.*, vol. 22, no. 4, pp. 1620–1630, Apr. 2013.

[3] Y. Romano, M. Protter, and M. Elad, "Single image interpolation via adaptive nonlocal sparsity-based modeling," *IEEE Trans. Image Process.*, vol. 23, no. 7, pp. 3085–3098, Jul. 2014.

[4] I. Ram, M. Elad, and I. Cohen, "Image processing using smooth ordering of its patches," *IEEE Trans. Image Process.*, vol. 22, no. 7, pp. 2764–2774, Jul. 2013.

[5] E. J. Candès and M. B. Wakin, "An introduction to compressive sampling," *IEEE Signal Process. Mag.*, vol. 25, no. 2, pp. 21–30, Apr. 2008.

[6] M. Fazel, "Matrix rank minimization with applications," Ph.D. dissertation, Elect. Eng. Dept., Stanford Univ., Stanford, CA, USA, 2002.

[7] E. J. Candès and T. Tao, "The power of convex relaxation: Near-optimal matrix completion," *IEEE Trans. Inf. Theory*, vol. 56, no. 5, pp. 2053–2080, Apr. 2010.

[8] Y. Hu, D. Zhang, J. Ye, X. Li, and X. He, "Fast and accurate matrix completion via truncated nuclear norm regularization," *IEEE Trans. Pattern Anal. Mach. Intell.*, vol. 35, no. 9, pp. 2117–2130, Sep. 2013.

[9] E. J. Candès and Y. Plan, "Matrix completion with noise," *Proc. IEEE*, vol. 98, no. 6, pp. 925–936, Jun. 2010.

[10] J.-F. Cai, E. J. Candès, and Z. Shen, "A singular value thresholding algorithm for matrix completion," *SIAM J. Opt.*, vol. 20, no. 4, pp. 1956–1982, 2010.

[11] S. Ma, D. Goldfarb, and L. Chen, "Fixed point and Bregman iterative methods for matrix rank minimization," *Math. Program.*, vol. 128, no. 1, pp. 321–353, 2011.

[12] K. C. Toh and S.W. Yun, "An accelerated proximal gradient algorithm for nuclear norm regularized least squares problems," *Pacific J. Optim.*, vol. 6, pp. 615–640, 2010.

[13] Z. Wen, W. Yin, and Y. Zhang, "Solving a low-rank factorization model for matrix completion by a nonlinear successive over-relaxation algorithm," *Math. Program. Comput.*, vol. 4, no. 4, pp. 333–361, 2012.

[14] P. Jain, P. Netrapalli, and S. Sanghavi, "Low-rank matrix completion using alternating minimization," in *Proc. 45th Annu. ACM Symp. Theory Comput.*, 2013, pp. 665–674.

[15] W. Dai and O. Milenkovic, "SET: An algorithm for consistent matrix completion," in *Proc. IEEE Int. Conf. Acoust., Speech, Signal Process.*, 2010, pp. 3646–3649.

[16] W. Gander and Q. Shi, "Matrix completion with ε-algorithm," *Numer. Algorithms*, vol. 80, no. 1, pp. 279–301, Jan. 2019.

[17] X. Jiang, Z. Zhong, X. Liu, and H. C. So, "Robust matrix completion via alternating projection," *IEEE Signal Process. Lett.*, vol. 24, no. 5, pp. 579–583, May 2017.

[18] Y.-X. Wang, C. M. Lee, L.-F. Cheong, and K.-C. Toh, "Practical matrix completion and corruption recovery using proximal alternating robust subspace minimization," *Int. J. Comput. Vision*, vol. 111, no. 3, pp. 315–344, Feb. 2015.

[19] Q. Zhao, D. Meng, Z. Xu, W. Zuo, and Y. Yan, "L1-Norm low-rank matrix factorization by variational Bayesian method," *IEEE Trans. Neural Netw. Learn. Syst.*, vol. 26, no. 4, pp. 825–839, Apr. 2015.

[20] J. Liu, P. Musialski, P. Wonka, and J. Ye, "Tensor completion for estimating missing values in visual data," *IEEE Trans. Pattern Anal. Mach. Intell.*, vol. 35, no. 1, pp. 208–220, Jan. 2013.

[21] L.T. Ko, J.E. Chen, Y.S. Shieh and T.Y. Sung, "A novel fractional discrete cosine transform based reversible watermarking for biomedical image applications," in *Proc. Int. Symp. Comput. Consum. Control*, Taichung, Taiwan, Jun. 2012, pp. 36–39.

[22] J. M. Hendrickx, A. Olshevsky, and V. Saligrama, "Minimax rank-1 factorization," in *Proc. 23rd Int. Conf. Artif. Intell. Statist.*, Palermo, Italy, Jun. 2020, pp. 1–21.

[23] W. J. Zeng and H. C. So, "Outlier-robust matrix completion via ℓ_p-minimization," *IEEE Trans. Signal Process.*, vol. 66, no. 5, pp. 1125–1140, Mar. 2018.

[24] P. Jain, P. Netrapalli, and S. Sanghavi, "Low-rank matrix completion using alternating minimization," in *Proc. 45th Annu. ACM Symp. Theory Comput.*, Palo Alto, CA, USA, Jun. 2013, pp. 665–674.

[25] D. P. O'Leary, "Robust regression computation using iteratively reweighted least squares," *SIAM J. Matrix Anal. Appl.*, vol. 11, no. 3, pp. 466–480, 1990.

[26] R. A. Maronna, R. D. Martin, and V. J. Yohai, *Robust Statistics: Theory and Methods.* New York, NY, USA: Wiley, 2006.

[27] Z. Wang, M.-J. Lai, Z. Lu, and J. Ye, "Orthogonal rank-one matrix pursuit for low rank matrix completion," *SIAM J. Sci. Comput.*, vol. 37, no. 1, pp. A488–A514, 2014.

[28] W.-J. Zeng, H. C. So, and L. Huang, "ℓ_p-MUSIC: Robust direction-of arrival estimator for impulsive noise environments," *IEEE Trans. Signal Process.*, vol. 61, no. 17, pp. 4296–4308, Sep. 2013.

[29] W.-J. Zeng, H. C. So, and X. Jiang, "Outlier-robust greedy pursuit algorithms in ℓ_p-space for sparse approximation," *IEEE Trans. Signal Process.*, vol. 64, no. 1, pp. 60–75, Jan. 2016.

[30] Q. Shi, H. Lu, and Y. M. Cheung, "Rank-one matrix completion with automatic rank estimation via l1-norm regularization," *IEEE Trans. Neural Netw. Learn. Syst.*, vol. 29, no. 10, pp. 4744–4757, Oct. 2018.